

Temperature statistics in turbulent Rayleigh–Bénard convection

J Lülff¹, M Wilczek and R Friedrich

Institute for Theoretical Physics, University of Münster,
Wilhelm-Klemm-Strasse 9, 48149 Münster, Germany
E-mail: johannes.luelff@uni-muenster.de

New Journal of Physics **13** (2011) 015002 (15pp)

Received 28 September 2010

Published 14 January 2011

Online at <http://www.njp.org/>

doi:10.1088/1367-2630/13/1/015002

Abstract. Rayleigh–Bénard (RB) convection in the turbulent regime is studied using statistical methods. Exact evolution equations for the probability density function of temperature and velocity are derived from first principles within the framework of the Lundgren–Monin–Novikov hierarchy known from homogeneous isotropic turbulence. The unclosed terms arising in the form of conditional averages are estimated from direct numerical simulations. Focusing on the statistics of temperature, the theoretical framework allows us to interpret the statistical results in an illustrative manner, giving deeper insights into the connection between dynamics and statistics of RB convection. The results are discussed in terms of typical flow features and the relation to the heat transfer.

Contents

1. Introduction	2
2. Single-point probability density function (PDF)	4
3. Single-point temperature PDF and implications of statistical symmetries	5
4. Connection to the heat transport	8
5. Numerical results	8
6. Summary	13
References	14

¹ Author to whom any correspondence should be addressed.

1. Introduction

Rayleigh–Bénard (RB) convection is a paradigm of a pattern-forming system far from equilibrium. Convective fluid motion in a vessel is induced by a vertical temperature gradient between the bottom and top boundaries due to buoyancy forces. In dependence on this temperature gradient, the geometry of the experiment and the fluid properties, a whole zoo of instabilities has been observed ranging from laminar, spatially coherent convective motion over spatially ordered but temporally chaotic up to highly turbulent fluid motion. See reviews available on the topic [1, 2].

Recently, much effort has been devoted to the analysis of turbulent RB convection by both experimental and theoretical means [3, 4]. Direct numerical simulations allow one to consider the dynamical and statistical properties of RB turbulence and the transitions between different types of flows in fine detail.

It is obvious that the analysis of turbulent convective fluid motion has to be based on a combination of tools from dynamical systems theory, statistical physics and the theory of stochastic processes. A necessary step is the statistical formulation of the underlying basic fluid dynamic equations, which for the most simple case are the Oberbeck–Boussinesq equations for the velocity field $\mathbf{u}(\mathbf{r}, t)$, the temperature field $T(\mathbf{r}, t)$ and the pressure field $p(\mathbf{r}, t)$,

$$\begin{aligned} \left[\frac{\partial}{\partial t} + \mathbf{u} \cdot \nabla \right] T(\mathbf{r}, t) &= \Delta T(\mathbf{r}, t), \\ \left[\frac{\partial}{\partial t} + \mathbf{u} \cdot \nabla \right] \mathbf{u}(\mathbf{r}, t) &= -\nabla p(\mathbf{r}, t) + Pr [\Delta \mathbf{u}(\mathbf{r}, t) + Ra T(\mathbf{r}, t) \mathbf{e}_z], \\ \nabla \cdot \mathbf{u}(\mathbf{r}, t) &= 0. \end{aligned} \quad (1.1)$$

The equations have been non-dimensionalized using the Rayleigh number $Ra = \alpha g \Delta T h^3 / \nu \kappa$, which is a dimensionless measure of the temperature gradient across the fluid layer (with thermal expansion coefficient α , gravitational acceleration g , outer temperature difference ΔT and distance of top and bottom plates h), as well as the Prandtl number $Pr = \frac{\nu}{\kappa}$ as the ratio of kinematic viscosity ν to heat conductivity κ of the fluid. Thus, the vertical spatial coordinate obeys $z \in [0, 1]$, and the boundary conditions of the temperature at the bottom and top plates are $T(z=0) = \frac{1}{2}$ and $T(z=1) = -\frac{1}{2}$. For the velocity, no-slip boundary conditions $\mathbf{u}(z=0) = \mathbf{u}(z=1) = 0$ are assumed. These equations are solved numerically by a suitably designed penalization approach, described in section 5. A snapshot of the temperature field is exhibited in figure 1.

The statistical analysis is based on joint probability density functions (PDFs) for the temperature and velocity at a single point in space and time. The basic fluid dynamic equations require the validity of certain relations among these PDFs. From these relations, corresponding expressions relating the various moments of the fields can be derived. For the case of incompressible turbulence, these relations have been formulated by Lundgren [6], Monin [7], Novikov [8], and Ulinich and Lyubimov [9] and are sometimes known as the Lundgren–Monin–Novikov (LMN) hierarchy. They are directly related to Hopf’s functional equation, which can be viewed as the basic statistical formulation of the Navier–Stokes equation in the Eulerian framework [10]. Similar relations can be derived for the corresponding

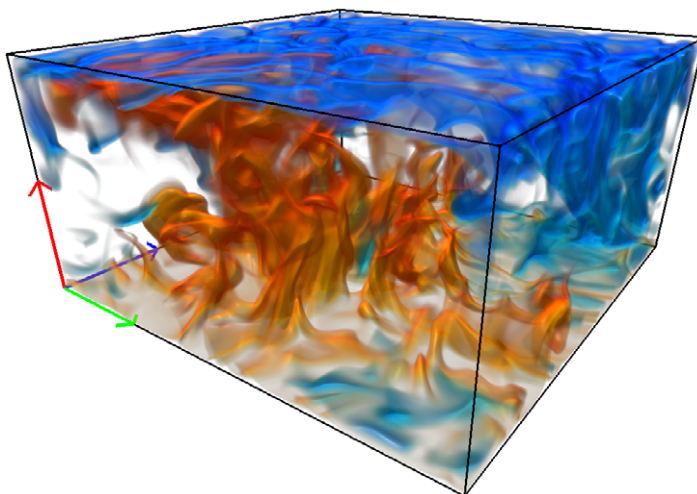


Figure 1. Snapshot of the temperature field $T(\mathbf{r})$. The green, blue and red arrows point in the x -, y - and z -directions, respectively. The volume rendering has been done with the open source renderer *Voreen* [5].

Lagrangian quantities [11]. It is evident that an analogous treatment is feasible for the Oberbeck–Boussinesq equations.

In this paper, we will use this approach in order to analyze the single-point temperature PDF for stationary turbulent RB convection. Our analysis combines direct numerical simulations with the relation of the LMN hierarchy for the single-point PDF. The result is a partial differential equation (PDE) for the temperature PDF. The derivation of this relation is outlined in section 2.

The aim is to formulate an equation that characterizes this PDF. Starting from the Oberbeck–Boussinesq equations, we derive an evolution equation for the single-point joint PDF of velocity and temperature along the lines of [6]–[8] for the case of incompressible turbulence. This equation is unclosed due to the fact that it contains unclosed expressions that can be related to fluid pressure, viscous dissipation and heat diffusion. However, these expressions can be treated by introducing conditional averages, which can be extracted from direct numerical simulations. This leads to a PDE for the joint temperature–velocity. A similar approach has been used by Novikov [12] and Novikov and Dommermuth [13], and more recently by Wilczek *et al* for the PDFs of vorticity [14] and velocity [15] for stationary, isotropic turbulence. On the other hand, modeling of unclosed terms is also a possible method, as used by e.g. Pope [16, 17]. As we shall indicate, the analysis of the evolution equation for the temperature PDF yields a comprehensive description of the dynamical processes in RB convection.

This paper is structured as follows. In section 2, we will derive the evolution equation for the temperature–velocity joint PDF. In section 3, we will reduce the joint PDF to the temperature PDF and make use of statistical symmetries to cut down the complexity of the evolution equation. Then we will present a descriptive way of dealing with this equation involving the method of characteristics. Section 4 will briefly discuss connections to the Nusselt number, relevant for the heat transport. These theoretical results are complemented by results from direct numerical simulations, which will be discussed in section 5, followed by a summary in section 6.

2. Single-point probability density function (PDF)

We are interested in the joint temperature–velocity probability distribution $f(\tau, \mathbf{v}; \mathbf{r}, t)$ and want to derive the corresponding evolution equation. Formally, the PDF is obtained as a suitable average over the so-called fine-grained probability distribution,

$$\widehat{f}(\tau, \mathbf{v}; \mathbf{r}, t) = \delta(\tau - T(\mathbf{r}, t)) \delta(\mathbf{v} - \mathbf{u}(\mathbf{r}, t)). \quad (2.1)$$

It is important to distinguish between *sample space* variables τ, \mathbf{v} and the corresponding *realizations* of the temperature and velocity fields $T(\mathbf{r}, t), \mathbf{u}(\mathbf{r}, t)$. Therefore, one could think of \widehat{f} as the PDF of one particular realization of the fields. Also, the notation of the arguments in $\widehat{f}(\tau, \mathbf{v}; \mathbf{r}, t)$ emphasizes the difference between the sample space variables τ, \mathbf{v} and the coordinates \mathbf{r}, t —the PDF is normalized with respect to the sample space variables, the coordinates are just parameters.

The full PDF is now obtained as an ensemble average over all possible realizations of the temperature and velocity fields,

$$f(\tau, \mathbf{v}; \mathbf{r}, t) = \langle \widehat{f}(\tau, \mathbf{v}; \mathbf{r}, t) \rangle = \langle \delta(\tau - T(\mathbf{r}, t)) \delta(\mathbf{v} - \mathbf{u}(\mathbf{r}, t)) \rangle. \quad (2.2)$$

The brackets $\langle \cdot \rangle$ denote the ensemble average, in contrast to spatial averages $\langle \cdot \rangle_V$ and $\langle \cdot \rangle_A$ over the whole fluid volume, or a horizontal plane at height z , respectively.

The definition of the fine-grained PDF (2.1) can be differentiated with respect to the space and time variables, giving

$$\frac{\partial}{\partial x_i} \widehat{f} = - \left[\frac{\partial}{\partial \tau} \frac{\partial T(\mathbf{r}, t)}{\partial x_i} \widehat{f} + \nabla_v \cdot \frac{\partial \mathbf{u}(\mathbf{r}, t)}{\partial x_i} \widehat{f} \right] \quad (2.3)$$

as the spatial gradient and an analogous equation for the temporal derivative $\frac{\partial}{\partial t} \widehat{f}$. Note that the operators $\frac{\partial}{\partial \tau}$ and ∇_v act on \widehat{f} . Now, multiplying (2.3) by u_i and adding the temporal derivative allows us to make use of the basic Oberbeck–Boussinesq equations (1.1). This results in the desired evolution equation for the fine-grained PDF,

$$\begin{aligned} \frac{\partial}{\partial t} \widehat{f} + \mathbf{u} \cdot \nabla \widehat{f} &= - \left[\frac{\partial}{\partial \tau} \left(\frac{\partial T}{\partial t} + \mathbf{u} \cdot \nabla T \right) \widehat{f} + \nabla_v \cdot \left(\frac{\partial \mathbf{u}}{\partial t} + \mathbf{u} \cdot \nabla \mathbf{u} \right) \widehat{f} \right] \\ &= - \frac{\partial}{\partial \tau} \Delta T \widehat{f} - \nabla_v \cdot [-\nabla p + Pr (\Delta \mathbf{u} + Ra T \mathbf{e}_z)] \widehat{f}. \end{aligned} \quad (2.4)$$

Performing the ensemble average of this equation in order to arrive at an equation for the full PDF (2.2), one encounters the closure problem of turbulence, since the unclosed averages $\langle \Delta T \widehat{f} \rangle$, $\langle -\nabla p \widehat{f} \rangle$ and $\langle \Delta \mathbf{u} \widehat{f} \rangle$ show up. The LMN *hierarchy* ansatz would mean to treat these terms via a coupling to the two-point PDF; the evolution equation of this two-point PDF would in turn introduce a coupling to the three-point PDF and so on [6].

Instead of introducing this hierarchy of coupled evolution equations for the multi-point PDFs, our strategy [14, 15] is to express the unclosed terms as conditional averages, since these are accessible to direct numerical simulations. The result is a PDE governing the joint temperature–velocity PDF and relating its shape as a function of space point \mathbf{r} to the conditional averages. The functional form of these conditional averages is a signature of the underlying dynamical processes of RB convection.

Introducing the conditional averages,

$$\begin{aligned}\langle \Delta T \widehat{f} \rangle &= \langle \Delta T | \tau, \mathbf{v}, \mathbf{r}, t \rangle f, \\ \langle -\nabla p \widehat{f} \rangle &= \langle -\nabla p | \tau, \mathbf{v}, \mathbf{r}, t \rangle f, \\ \langle \Delta \mathbf{u} \widehat{f} \rangle &= \langle \Delta \mathbf{u} | \tau, \mathbf{v}, \mathbf{r}, t \rangle f,\end{aligned}\tag{2.5}$$

we arrive at the following relation for the single-point probability distribution $f(\tau, \mathbf{v}; \mathbf{r}, t)$,

$$\begin{aligned}\frac{\partial}{\partial t} f + \mathbf{v} \cdot \nabla f &= -\frac{\partial}{\partial \tau} \langle \Delta T | \tau, \mathbf{v}, \mathbf{r}, t \rangle f \\ &\quad - \nabla_{\mathbf{v}} \cdot [\langle -\nabla p | \tau, \mathbf{v}, \mathbf{r}, t \rangle + Pr (\langle \Delta \mathbf{u} | \tau, \mathbf{v}, \mathbf{r}, t \rangle + Ra\tau \mathbf{e}_z)] f.\end{aligned}\tag{2.6}$$

Since at the boundaries of the RB cell the velocity and temperature fields are statistically sharp quantities, the probability distribution has to obey the conditions $f(\tau, \mathbf{v}; z=0) = \delta(\tau - \frac{1}{2})\delta(\mathbf{v})$ and $f(\tau, \mathbf{v}; z=1) = \delta(\tau + \frac{1}{2})\delta(\mathbf{v})$ for arbitrary x, y .

We note in passing that a different version of the evolution equation can be obtained by introducing the Laplacian of the PDF. Specializing in the case $Pr = 1$, it is possible to re-express the conditional averages $\langle \Delta T | \tau, \mathbf{v}, \mathbf{r}, t \rangle$ and $\langle \Delta \mathbf{u} | \tau, \mathbf{v}, \mathbf{r}, t \rangle$ via the relation

$$\begin{aligned}\Delta f &= -\frac{\partial}{\partial \tau} \langle \Delta T \widehat{f} \rangle - \nabla_{\mathbf{v}} \cdot \langle \Delta \mathbf{u} \widehat{f} \rangle \\ &\quad + \frac{\partial^2}{\partial \tau^2} \langle (\nabla T)^2 \widehat{f} \rangle + 2 \frac{\partial^2}{\partial \tau \partial v_j} \langle \nabla T \cdot \nabla u_j \widehat{f} \rangle + \frac{\partial^2}{\partial v_i \partial v_j} \langle \nabla u_i \cdot \nabla u_j \widehat{f} \rangle.\end{aligned}\tag{2.7}$$

Here and in the following, Einstein's summation convention over repeated indices is used. Again, we can introduce conditional expectations, where the arguments of the conditional averages have been abbreviated as $\star \hat{=} \tau, \mathbf{v}, \mathbf{r}, t$. The resulting evolution equation reads

$$\begin{aligned}\frac{\partial}{\partial t} f + \mathbf{v} \cdot \nabla f &= \Delta f - \nabla_{\mathbf{v}} \cdot [\langle -\nabla p | \star \rangle + Ra\tau \mathbf{e}_z] f - \frac{\partial^2}{\partial \tau^2} \langle (\nabla T)^2 | \star \rangle f \\ &\quad - 2 \frac{\partial^2}{\partial \tau \partial v_j} \langle \nabla T \cdot \nabla u_j | \star \rangle f - \frac{\partial^2}{\partial v_i \partial v_j} \langle \nabla u_i \cdot \nabla u_j | \star \rangle f.\end{aligned}\tag{2.8}$$

A somewhat more complicated equation holds for $Pr \neq 1$. This relationship shows that the single-point joint temperature–velocity PDF $f(\tau, \mathbf{v}; \mathbf{r}, t)$ is essentially determined by the conditionally averaged dissipation-like terms $\langle (\nabla T)^2 | \star \rangle$, $\langle \nabla T \cdot \nabla u_j | \star \rangle$ and $\langle \nabla u_i \cdot \nabla u_j | \star \rangle$ as well as the conditional pressure gradient $\langle -\nabla p | \star \rangle$.

3. Single-point temperature PDF and implications of statistical symmetries

In the following, we shall restrict our attention to the reduced temperature probability distribution and its evolution equation. As it will turn out, already this equation gives insights into the connection between RB dynamics and temperature statistics, besides obviously describing the temperature statistics. Also, because the final evolution equation of temperature PDF involves scalar valued functions only, a numerical approach is easily feasible.

The reduced temperature PDF is obtained by integrating out the velocity part,

$$h(\tau; \mathbf{r}, t) = \int d^3v f(\tau, \mathbf{v}; \mathbf{r}, t).\tag{3.1}$$

Starting from equation (2.6), we obtain the simple equation

$$\frac{\partial}{\partial t} h + \nabla \cdot \langle \mathbf{u} | \tau, \mathbf{r}, t \rangle h = - \frac{\partial}{\partial \tau} \langle \Delta T | \tau, \mathbf{r}, t \rangle h, \quad (3.2)$$

where we have performed the integration with respect to the velocity \mathbf{v} . Thereby, we had to introduce the conditional averages $\langle \mathbf{u} | \tau, \mathbf{r}, t \rangle$ and $\langle \Delta T | \tau, \mathbf{r}, t \rangle$. Alternatively, one could re-enact the derivation performed in section 2 for the fine-grained PDF of the temperature $\widehat{h}(\tau; \mathbf{r}, t) = \delta(\tau - T(\mathbf{r}, t))$.

Analogous to (2.8), we can derive a further relation using the identity

$$\Delta h = \langle \Delta \widehat{h} \rangle = - \frac{\partial}{\partial \tau} \langle \Delta T(\mathbf{r}, t) \widehat{h} \rangle + \frac{\partial^2}{\partial \tau^2} \langle (\nabla T(\mathbf{r}, t))^2 \widehat{h} \rangle. \quad (3.3)$$

This relation also follows from (2.7). With this equation, we can now summarize the equation for the temperature PDF $h(\tau; \mathbf{r}, t)$ in the form

$$\frac{\partial}{\partial t} h + \nabla \cdot \langle \mathbf{u} | \tau, \mathbf{r}, t \rangle h = \Delta h - \frac{\partial^2}{\partial \tau^2} \langle (\nabla T)^2 | \tau, \mathbf{r}, t \rangle h. \quad (3.4)$$

Here, the conditional average of the term $(\nabla T)^2$ comes up, which is related to the Nusselt number. The details will be discussed in section 4.

The evaluation of the conditional averages appearing in (3.2) is greatly simplified by considering convection that is statistically stationary in time and has periodic horizontal boundaries (i.e. is homogeneous with respect to the horizontal coordinates). Under the assumption of a statistically stationary flow, the PDFs and therefore the conditional averages cannot depend on the time variable; also, the dependence on the horizontal coordinates drops out. Hence, instead of dealing with statistical quantities that depend on \mathbf{r} and t , we simply have to retain the z -dependence.

Let us first consider the determining equation for the temperature PDF $h(\tau; z)$ in the form

$$\frac{\partial}{\partial z} \langle u_z | \tau, z \rangle h(\tau; z) + \frac{\partial}{\partial \tau} \langle \Delta T | \tau, z \rangle h(\tau; z) = 0, \quad (3.5)$$

obtained from (3.2). This equation in principle has to be solved together with the boundary conditions $h(\tau; 0) = \delta(\tau - \frac{1}{2})$ and $h(\tau; 1) = \delta(\tau + \frac{1}{2})$ and with appropriately modeled expressions for the conditional averages $\langle u_z | \tau, z \rangle$ and $\langle \Delta T | \tau, z \rangle$. This direct approach will not be conducted in the present paper, however, but can be taken as a starting point for future modeling.

Instead, this first-order PDE can be analyzed with the help of the method of characteristics [18]. Applying this method, one can find curves $(\tau(s), z(s))$ in the τ - z phase space parameterized by s along which the PDE (3.5) transforms into an ordinary differential equation, which can be integrated. This approach will be sketched in the following.

Writing $h(s) = h(\tau(s); z(s))$ and calculating the derivative of it gives

$$\frac{d}{ds} h(\tau(s), z(s)) = \frac{\partial h}{\partial \tau} \frac{d\tau}{ds} + \frac{\partial h}{\partial z} \frac{dz}{ds}. \quad (3.6)$$

The PDE (3.5) is re-expressed in the form

$$\langle \Delta T | \tau, z \rangle \frac{\partial h}{\partial \tau} + \langle u_z | \tau, z \rangle \frac{\partial h}{\partial z} = - \left(\frac{\partial}{\partial \tau} \langle \Delta T | \tau, z \rangle + \frac{\partial}{\partial z} \langle u_z | \tau, z \rangle \right) h. \quad (3.7)$$

Comparing these two equations identifies the characteristic curves as the solutions of

$$\begin{aligned}\frac{d}{ds}\tau &= \langle \Delta T | \tau, z \rangle, \\ \frac{d}{ds}z &= \langle u_z | \tau, z \rangle.\end{aligned}\tag{3.8}$$

Along these curves, the PDE (3.5) becomes

$$\frac{d}{ds}h = - \left(\frac{\partial}{\partial \tau} \langle \Delta T | \tau, z \rangle + \frac{\partial}{\partial z} \langle u_z | \tau, z \rangle \right) h,\tag{3.9}$$

which can be integrated to

$$h(s) = h(s_0) \exp \left[- \int_{s_0}^s ds \left(\frac{\partial}{\partial \tau} \langle \Delta T | \tau, z \rangle + \frac{\partial}{\partial z} \langle u_z | \tau, z \rangle \right) \right].\tag{3.10}$$

This equation describes the evolution of the PDF along a trajectory $(\tau(s), z(s))$ starting at the point $(\tau(s_0), z(s_0))$ in phase space. A particularly appealing property of this formalism is that it allows us to interpret the statistical results in an illustrative manner, because the characteristics, i.e. trajectories in τ - z phase space, show the evolution of the ‘averaged’ physical process.

It is tempting to interpret the characteristics as a kind of Lagrangian dynamics of a tracer particle inside the RB cell. However, the dynamics of a tracer particle are stochastic, whereas the characteristics defined by (3.8) describe purely deterministic trajectories and, thus, take the stochastic properties into account only in an averaged way. In a sense, the characteristics describe the averaged evolution of an ensemble of fluid particles that are defined by their initial condition in the τ - z -plane.

Thinking of turbulent RB convection with some physical intuition, one can expect certain features from the statistical quantities introduced in this section. The conditionally averaged vertical velocity $\langle u_z | \tau, z \rangle$ should show positive correlation with the temperature, i.e. it should mirror the well-known fact that hot fluid rises up and cold fluid sinks down. Also the no-slip boundaries should be recognizable for $z \approx 0$ and $z \approx 1$, respectively. The absolute value of the heat diffusive term $\langle \Delta T | \tau, z \rangle$ should be highest near the boundaries because of the sharp change in the temperature profile. As the characteristics in a way describe the average path that a fluid particle takes through τ - z phase space, the typical RB cycle of fluid heating up at the bottom, rising up, cooling down at the top and sinking down again should find its correspondence in the statistical quantities describing the evolution of the PDF. Actual numerical studies of these quantities will be discussed in detail in section 5.

In the 1990s, an approach similar to the presented one here was used by V Yakhot and followers, where PDFs of various quantities in a stationary flow were expressed as integrals over conditionally averaged variables. The considered quantities included passive scalars by Sinai and Yakhot [19], an active scalar, such as temperature fluctuations by Yakhot [20] and temperature increments by Ching [21], and even general functions of an arbitrary quantity measured in the flow by Pope and Ching [22, 23]. The conditional averages included spatial and temporal derivatives of these quantities.

In contrast to these works, we do not assume homogeneity in the spatial coordinates, i.e. we still have the z -dependence present in our PDF equations. This allows us to discuss the

PDFs with respect to the z -coordinate and observe qualitatively different statistics in different regions of the flow. As a result, we are able to see the differing behavior of bulk and boundary parts of the convection cell and how these are connected to the conditional averages and their dependence on the vertical position. This has not been addressed in the literature.

4. Connection to the heat transport

The Nusselt number Nu as the ratio of convective to conductive heat transfer plays a key role in the analysis of RB convection. It serves as a measure of how efficiently heat can be transported through the convection cell.

Although we have not considered the Nusselt number so far, we note that there is an interesting connection between Nu and the conditional averages that appear in our calculations. Because the Nusselt number may be defined as the volume average $Nu = \langle (\nabla T)^2 \rangle_V$ in non-dimensional units, the following expression comes up,

$$Nu = \frac{1}{V} \int d^3r \, d\tau \langle (\nabla T)^2 | \tau, \mathbf{r} \rangle h(\tau; \mathbf{r}). \quad (4.1)$$

Therefore, $\langle (\nabla T)^2 | \tau, \mathbf{r} \rangle$ can be viewed as a conditional Nusselt number density. We point out that this quantity should be of considerable interest for the evaluation of theories concerning the Rayleigh number dependence of the Nusselt number based on a decomposition of the heat transport into bulk and boundary contributions, which underlies the Grossmann–Lohse theory [24] outlined in the review of Ahlers *et al* [4]. Also, this term is linked to the temperature dissipation rate, which is discussed in [25] with respect to temperature PDFs.

In a similar manner, we can employ the temperature–velocity joint PDF $f(\tau, \mathbf{v}; \mathbf{r})$ to derive an equation relating the Rayleigh and the Nusselt numbers. From the relation $Ra(Nu - 1) = \langle (\nabla \mathbf{u})^2 \rangle_V$, it is straightforward to see that

$$\int d^3r \, d\tau \, d^3v \, f(\tau, \mathbf{v}; \mathbf{r}) [Ra \langle (\nabla T)^2 | \tau, \mathbf{v}, \mathbf{r} \rangle - 1 - \langle (\nabla \mathbf{u})^2 | \tau, \mathbf{v}, \mathbf{r} \rangle] = 0. \quad (4.2)$$

These two exact relations underline the importance of the conditional averages of $(\nabla T)^2$ and $(\nabla \mathbf{u})^2$ that naturally come up in our derivations.

5. Numerical results

The benefit of our theoretical approach is that we can easily provide it with measurements and data in the form of numerical results. To this end, we solve the basic Oberbeck–Boussinesq equations (1.1) with a standard dealiased pseudospectral code on a three-dimensional (3D) equidistant Cartesian grid with periodic boundary conditions. For an introduction to this topic, see [26, 27].

Periodic boundaries are required in the horizontal direction, whereas in the vertical direction Dirichlet conditions for velocity and temperature (i.e. no-slip boundaries of constant temperature) are needed. They are enforced by a *volume penalization ansatz* [28]–[30]: the fluid domain $\Omega = [0, L_x] \times [0, L_y] \times [0, 1] \subset \mathbb{R}^3$ is embedded in a computational domain that is extended by a layer of thickness d in the z -direction, $\Omega_c = [0, L_x] \times [0, L_y] \times [-d, 1+d]$.

Inside the fluid domain $\Omega \subset \Omega_c$ the unaltered Oberbeck–Boussinesq equations are solved, whereas in the appended extra regions $\Omega_c \setminus \Omega$ a strong exponential damping ($-\frac{1}{\eta} \mathbf{u}$ and $-\frac{1}{\eta} \theta$, respectively, with $\eta \ll 1$) is added to the evolution equations (1.1) of velocity and temperature that damps the fields to zero. By simulating the deviation from the linear temperature profile, $\theta(\mathbf{r}, t) := T(\mathbf{r}, t) + (z - \frac{1}{2})$, instead of the temperature itself, the desired boundary conditions read $\mathbf{u} = 0$ and $\theta = 0$ for $z = 0$ and $z = 1$. This change in variables $T \rightarrow \theta$ allows us to make use of the volume penalization approach in a straightforward manner.

The reason we choose this numerical scheme instead of the often used Chebyshev-based codes, described for example in [26] and used in e.g. [31, 32], is because it allows for almost arbitrary shaped boundaries and sidewalls. Although this feature is not used in the present paper due to the required horizontal homogeneity, it even allows us to simulate cylindrical vessels on a (numerically cheap) Cartesian grid. A more detailed report on this will be published in the future.

Our theoretical derivation relies on the concept of ensemble averages. Of course, through our numerics we can only access a finite subset of all possible ensemble members. So due to the statistical symmetries and by assuming ergodicity, the ensemble average is substituted for a combined volume–time average in the numerics. Likewise, the volume-averages $\langle \cdot \rangle_V$ and $\langle \cdot \rangle_A$ introduced earlier are actually evaluated as combined volume and time averages. Here, time averaging means averaging over 1250 statistically independent snapshots of the fields. The line plots below only show the parts of the statistical quantities where the statistics converged, i.e. where a significant number of events were obtained.

The simulation was conducted for the parameters $Ra = 4.33 \times 10^7$ and $Pr = 1$. The computational domain Ω_c is resolved with $N_x \times N_y \times N_z = 256 \times 256 \times 192$ gridpoints on an equidistant Cartesian grid, where the fluid domain $\Omega \subset \Omega_c$ is represented by $256 \times 256 \times 128$ gridpoints. Thus, the aspect ratio is $\Gamma = 2$, with the two horizontal dimensions being identical. The Nusselt number is estimated to be $Nu = 24.2$. We mention that we repeated the analysis presented below with a simulation of aspect ratio $\Gamma = 4$ and found basically the same features, due to the fact that for sufficiently large Γ the periodic boundaries do not have a significant influence on the flow.

Figure 2(a) shows the color-coded temperature PDF $h(\tau; z)$ in a logarithmic plot, where the black and gray lines indicate the mean temperature profile $\langle T(z) \rangle_A$ and the square root of the centralized second moment, $\langle (T - \langle T(z) \rangle_A)^2 \rangle_A^{1/2}$, i.e. standard deviation. Figure 2(b) shows slices in the τ -direction indicated by the dashed lines in figure 2(a). In the color plot, one clearly observes the sharp change in the temperature PDF from a δ -function at the boundaries across the boundary layer to a shape exhibiting larger tails in the bulk. In addition to these tails, another feature of the PDF is the hump close to the $\tau = 0$ -line. This hump corresponds to the most probable value of the temperature. One expects two different dynamical features to be responsible for this special shape; a tempting explanation would be to attribute the hump to the background temperature field of mean temperature, and account the wings for large $|\tau|$ for plumes that carry fluid that is much colder or hotter than the surrounding fluid. Evidence for this is the shape of the PDF close to the bottom or top boundaries (but still outside the boundary layers): at $z = 4\delta_T$, although the most probable temperature value is moved slightly toward lower temperatures, the PDF exhibits a large tail at high temperatures. The interpretation is that mostly cold fluid gathers in the lower regions of the bulk, being almost at rest (compare the region of $\langle u_z | \tau, z = 4\delta_T \rangle$ in figure 3(b) corresponding to the hump), while very hot fluid is a more rare event, because hot fluid is convected away quickly due to plume dynamics.

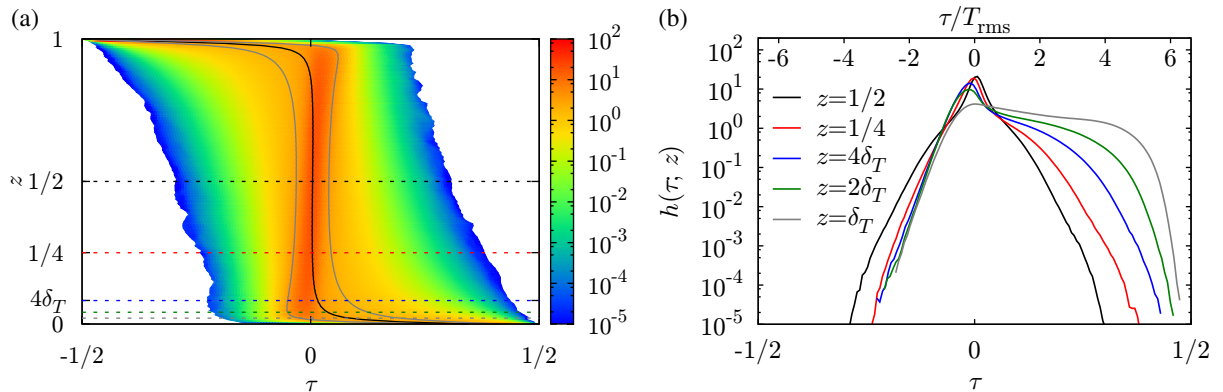


Figure 2. (a) The mean temperature $\langle T(z) \rangle_A$ and a color plot of the logarithm of the temperature PDF $h(\tau; z)$ as a function of z . The additional solid gray lines mark the contour line for $\langle T(z) \rangle_A \pm \langle (T - \langle T(z) \rangle_A)^2 \rangle_A^{1/2}$ and indicate the standard deviation of temperature at height z . The horizontal dashed lines indicate the positions of slices in the τ -direction at fixed height and are located at $z \in \{\frac{1}{2}, \frac{1}{4}, 4\delta_T, 2\delta_T, \delta_T\}$, where $\delta_T = \frac{1}{2Nu}$ is the thermal boundary layer thickness. (b) The logarithm of the temperature PDF $h(\tau; z)$ for different values of z . The upper abscissa is scaled in units of the globally taken standard deviation of temperature, $T_{\text{rms}} = \sqrt{\langle T^2 \rangle_V}$.

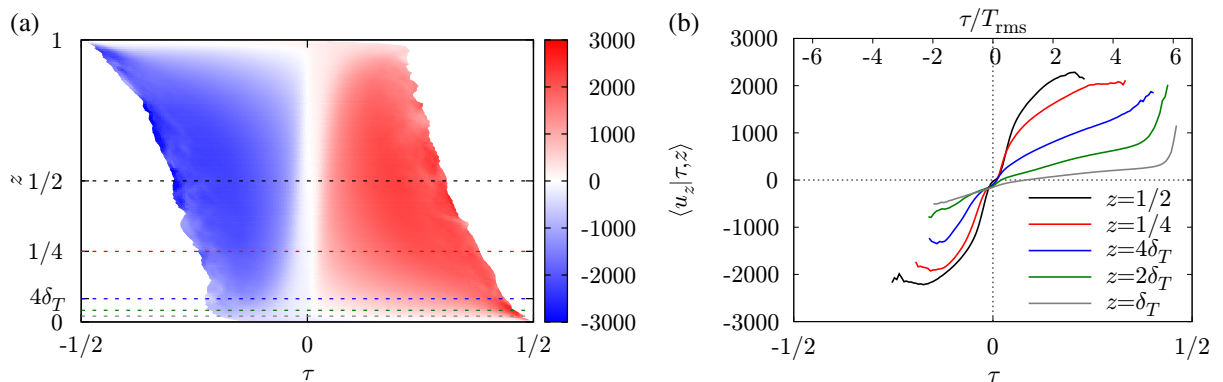


Figure 3. (a) Color plot of the conditional velocity field $\langle u_z | \tau, z \rangle$, with dashed lines as in figure 2. Due to the non-dimensionalization, the velocity is given in units of the heat diffusion velocity, i.e. the velocity with which heat would be transported from plate to plate by pure heat diffusion. (b) The conditional velocity field $\langle u_z | \tau, z \rangle$ as a function of τ for various values of z .

The reason why the hot fluid takes greater temperature values than the cold fluid (in terms of absolute value) is that very cold fluid detaching from the top plate already heats up on its way down.

PDFs of the same shape for Rayleigh numbers of the same order are reported in [25], where also the dependence on the vertical coordinate is taken into account. The experimental data in [21, 33] show a more pronounced exponential shape of the temperature PDF, which can be attributed to the difference in the Rayleigh numbers which are several orders of magnitude

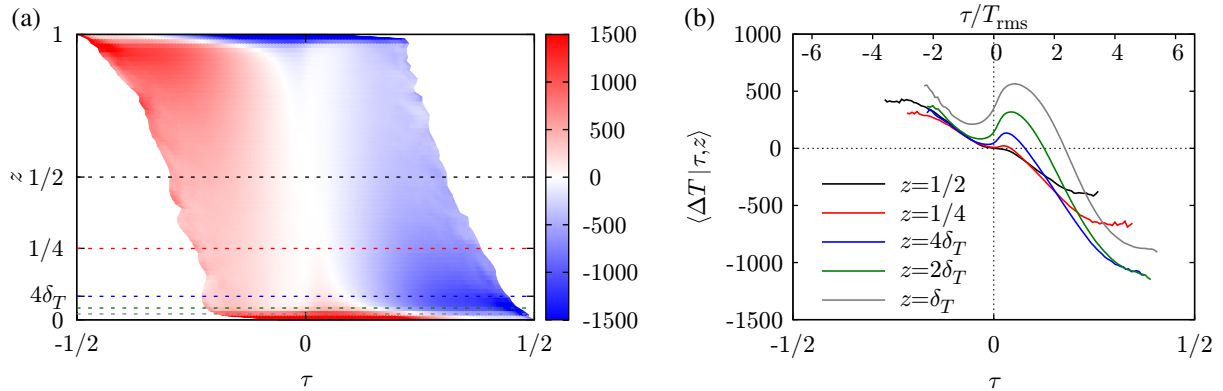


Figure 4. (a) Color plot of the conditional heat diffusion field $\langle \Delta T | \tau, z \rangle$, with dashed lines as in figure 2. (b) The conditional heat diffusion field $\langle \Delta T | \tau, z \rangle$ as a function of τ for various values of z .

above ours; the numerical data in [25] suggest that the PDFs become more exponential with increasing Rayleigh number.

Figures 3 and 4 exhibit the conditional averages introduced in section 3. One can clearly observe the features that were suggested in the aforementioned section. The conditional vertical velocity $\langle u_z | \tau, z \rangle$ is high (low) for hot (cold) fluid, respectively, and the no-slip boundary conditions manifest in the fact that $\langle u_z | \tau, z \rangle$ is close to zero for $z \approx 0$ and $z \approx 1$. Additionally, one observes a stripe close to the $\tau = 0$ -line of almost vanishing vertical velocity, which coincides with the reddish core (the hump, i.e. the most probable value) of the temperature PDF in figure 2(a). The interpretation is that fluid that is as hot as the mean temperature is neutrally buoyant and neither moves up nor moves down. Another striking feature is the sudden increase in the vertical velocity for high τ near the boundary layer, i.e. for $z = \delta_T$, which we attribute to rising plumes that detach from the hot bottom plate. Again, it must be stressed that these interpretations hold in an averaged sense.

Figure 4 shows that the conditional heat diffusion term $\langle \Delta T | \tau, z \rangle$ is (in terms of absolute value) highest at the boundaries, with the term being positive (negative) at the hot bottom (cold top) plate. In contrast, in the bulk the absolute value is high (low) for very cold (hot) fluid, i.e. in the wings of the temperature PDF. Additionally, the τ -slice near the boundary in figure 4(b) shows an under- and overshoot. The connection of these unique features to the RB dynamics has yet to be understood.

By combining the two aforementioned conditional averages to the vector field (3.8) that defines the characteristics as suggested in section 3, one arrives at the vector field depicted in figure 5—one of our central results. It is easy to interpret this graph by tracing the vector field; one can qualitatively reconstruct the typical RB cycle of fluid heating up at the bottom, rising up while starting to cool down, cooling down drastically at the top plate, falling down towards the bottom plate while warming up a bit and heating up again at the bottom. It is especially illustrative to see that the main contribution of cooling and heating (i.e. the biggest movement in the τ -direction of phase space) takes place near the boundaries, highlighting the importance of the boundary layers, while obviously the biggest movement in the z -direction occurs in the bulk.

Yet one has to consider, for example, that although hot fluid rises up very quickly (referring to the vectors pointing upwards at the right side in figure 5), this does not contribute much to

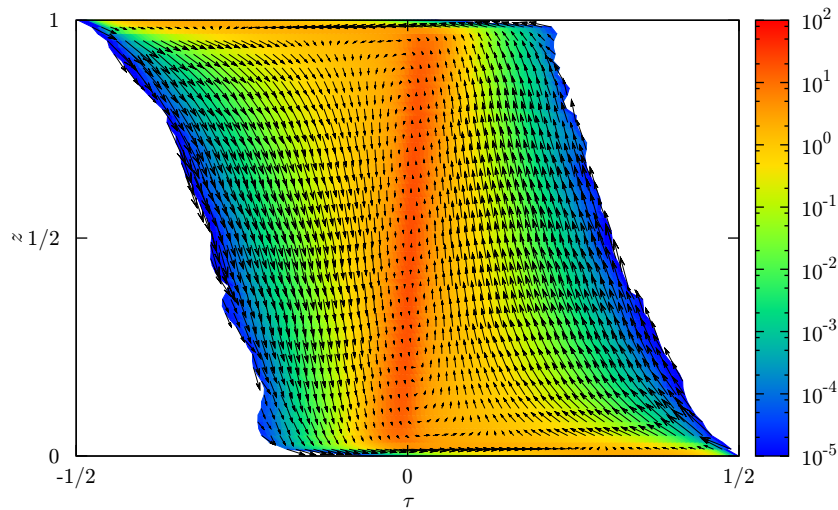


Figure 5. Color plot of the temperature PDF $h(\tau; z)$ together with the vector field identifying the characteristics.

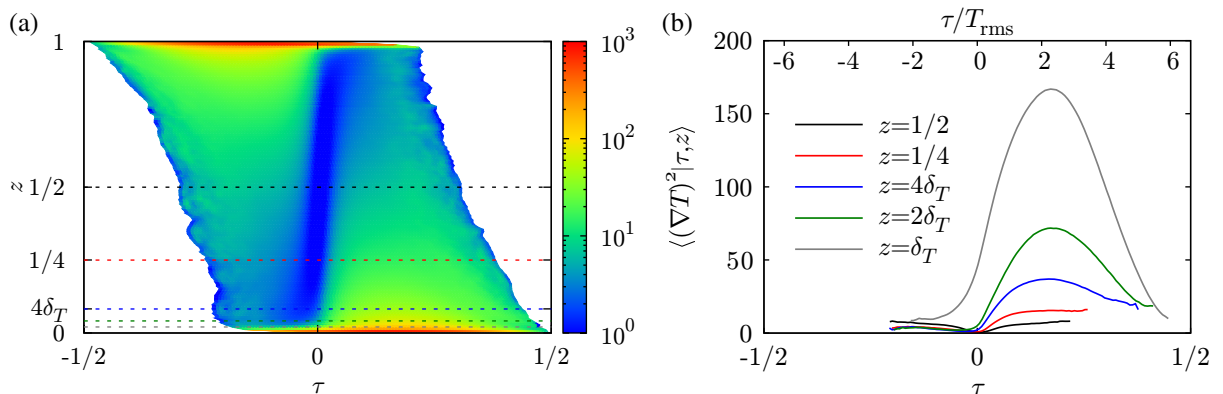


Figure 6. (a) Color plot of the conditional field $\langle (\nabla T)^2 | \tau, z \rangle$, with dashed lines as in figure 2. The color axis is scaled logarithmically. (b) The field $\langle (\nabla T)^2 | \tau, z \rangle$ as a function of τ for various values of z .

heat transport because these events occur rarely, as indicated by the temperature PDF shown along with the vector field governing the characteristics.

In figure 6, the conditional heat dissipation rate $\langle (\nabla T)^2 | \tau, z \rangle$ is shown, which can be interpreted as a Nusselt number density according to (4.1). The notable features are a pronounced minimum near the most probable temperature, again coinciding with the reddish core of the PDF. Also, in the boundary layer this quantity attains huge values (note the logarithmic scaling in the color plot), which highlights the fact that the boundary layer contributes much to the heat transport. A similar shape of a related quantity is reported in [25] (using the deviation from the mean temperature profile instead of the temperature itself), although there the conditional average is taken over the whole fluid volume and is hence lacking the z -dependence.

6. Summary

In this paper, we have analyzed the single-point temperature PDF on the basis of the LMN hierarchy by truncating the hierarchy on the first level via the introduction of conditional averages.

We first derived the evolution equation of the full joint PDF of temperature and velocity. Then we focused on the temperature PDF only, which is the central point of this paper, and obtained an evolution equation for it by reducing the joint PDF equation. We assumed rather weak symmetry conditions of statistical stationarity in time and homogeneity in lateral spatial directions; these conditions should be fulfilled at reasonably high aspect ratios even for closed vessels, i.e. they are a good approximation of experimental setups in the bulk of the flow. Under these symmetry considerations, the evolution equation of the temperature PDF becomes fairly simple. The arising conditional averages of temperature diffusion $\langle \Delta T | \tau, z \rangle$ and vertical velocity $\langle u_z | \tau, z \rangle$ are estimated by direct numerical simulations using a suitably designed penalization approach, and features of them are discussed. This shows that expected features, such as the properties of the temperature and velocity boundary layers, correlation of temperature and velocity and so on, are related to the form of these conditional averages that naturally come up in our derivations.

The evolution equation of the temperature PDF is readily treated by the method of characteristics. Due to the applied symmetry conditions, the phase space that describes our system becomes 2D, spanned by temperature τ and the vertical coordinate z . Because of this reduced dimensionality of the system, the method of characteristics yields a descriptive view of the RB dynamics, resulting in the vector field describing the evolution in τ - z phase space. The characteristics, i.e. trajectories in τ - z phase space, are found to reproduce the typical cycle of a fluid parcel. The regions of the main transport in the τ -direction have been identified as the boundary layers, while the major movement in the z -direction takes place in the bulk. This highlights the importance of the boundary layers to the heat transport. The relation of heat transport in terms of the Nusselt number to the conditional averages introduced in our derivation is briefly discussed, leading us to the definition of a Nusselt number density. It would be very interesting to obtain the statistical quantities describing the evolution of the PDF directly from experiments, e.g. from measurements of instrumented particles, as described in [34].

Future effort will be aimed at not only using the characteristics as an illustrative way to describe the mean movement in phase space but also actually calculating the PDF of temperature from the integral representation (3.10). Also, modeling of the conditional averages, which are until now estimated from direct numerical simulations, might be feasible; an intermediate step would be to discuss the quantities not in the turbulent case but close above the bifurcation from heat conduction to convection, where analytical solutions of temperature and velocity fields are available. Although an easy illustration in the form of trajectories in 2D space will not be achievable in the case of the joint PDF, this approach is nevertheless promising and planned for the future, because we hope that already the form of the conditional averages will give insights into the connection of the statistics to the RB dynamics. An intermediate step would be to concentrate on the joint PDF of temperature and vertical velocity, which should among others relate to the dynamics of plumes.

References

- [1] Busse F H 1978 Non-linear properties of thermal convection *Rep. Prog. Phys.* **41** 1929–67
- [2] Bodenschatz E, Pesch W and Ahlers G 2000 Recent developments in Rayleigh–Bénard convection *Annu. Rev. Fluid Mech.* **32** 709–78
- [3] Siggia E D 1994 High Rayleigh number convection *Annu. Rev. Fluid Mech.* **26** 137–68
- [4] Ahlers G, Grossmann S and Lohse D 2009 Heat transfer and large scale dynamics in turbulent Rayleigh–Bénard convection *Rev. Mod. Phys.* **81** 503–37
- [5] Meyer-Spradow J, Ropinski T, Mensmann J and Hinrichs K H 2009 Voreen: a rapid-prototyping environment for ray-casting-based volume visualizations *IEEE Comput. Graph. Appl.* **29** 6–13
- [6] Lundgren T S 1967 Distribution functions in the statistical theory of turbulence *Phys. Fluids* **10** 969–75
- [7] Monin A S 1967 Equations of turbulent motion *Prikl. Mat. Mekh.* **31** 1057–68
- [8] Novikov E A 1968 Kinetic equations for a vortex field *Sov. Phys.—Dokl.* **12** 1006–8
- [9] Ulinich F R and Lyubimov B Y 1968 The statistical theory of turbulence in an incompressible fluid for large Reynolds numbers *Sov. Phys.—JETP* **28** 494–500
- [10] Monin A S and Yaglom A M 2007 *Statistical Fluid Mechanics: Mechanics of Turbulence* (New York: Dover)
- [11] Friedrich R 2003 Statistics of Lagrangian velocities in turbulent flows *Phys. Rev. Lett.* **90** 084501
- [12] Novikov E A 1993 A new approach to the problem of turbulence, based on the conditionally averaged Navier–Stokes equations *Fluid Dyn. Res.* **12** 107–26
- [13] Novikov E A and Dommermuth D G 1994 Conditionally averaged dynamics of turbulence *Mod. Phys. Lett. B* **8** 1395–401
- [14] Wilczek M and Friedrich R 2009 Dynamical origins for non-Gaussian vorticity distributions in turbulent flows *Phys. Rev. E* **80** 016316
- [15] Wilczek M, Daitche A and Friedrich R 2010 On the velocity distribution in homogeneous isotropic turbulence: correlations and deviations from Gaussianity *J. Fluid Mech.* (submitted)
- [16] Pope S B 1981 Transport equation for the joint probability density function of velocity and scalars in turbulent flow *Phys. Fluids* **24** 588–96
- [17] Pope S B 2000 *Turbulent Flows* (Cambridge: Cambridge University Press)
- [18] Courant R and Hilbert D 1962 *Methods of Mathematical Physics* vol II (New York: Wiley-Interscience)
- [19] Sinai Ya G and Yakhot V 1989 Limiting probability distributions of a passive scalar in a random velocity field *Phys. Rev. Lett.* **63** 1962–4
- [20] Yakhot V 1989 Probability distributions in high-Rayleigh number Bénard convection *Phys. Rev. Lett.* **63** 1965–7
- [21] Ching E S C 1993 Probability densities of turbulent temperature fluctuations *Phys. Rev. Lett.* **70** 283–6
- [22] Pope S B and Ching E S C 1993 Stationary probability density functions: an exact result *Phys. Fluids A: Fluid Dyn.* **5** 1529–31
- [23] Ching E S C 1996 General formula for stationary or statistically homogeneous probability density functions *Phys. Rev. E* **53** 5899–03
- [24] Grossmann S and Lohse D 2000 Scaling in thermal convection: a unifying theory *J. Fluid Mech.* **407** 27–56
- [25] Emran M S and Schumacher J 2008 Fine-scale statistics of temperature and its derivatives in convective turbulence *J. Fluid Mech.* **611** 13–34
- [26] Boyd J P 2001 *Chebyshev and Fourier Spectral Methods* 2nd revised edn (New York: Dover)
- [27] Canuto C, Hussaini M Y, Quarteroni A and Zang T A 1987 *Spectral Methods in Fluid Dynamics* (Berlin: Springer)
- [28] Angot P, Bruneau C-H and Fabrie P 1999 A penalization method to take into account obstacles in incompressible viscous flows *Numer. Math.* **81** 497–520
- [29] Schneider K 2005 Numerical simulation of the transient flow behaviour in chemical reactors using a penalisation method *Comput. Fluids* **34** 1223–38

- [30] Keetels G H, D'Ortona U, Kramer W, Clercx H J H, Schneider K and van Heijst G J F 2007 Fourier spectral and wavelet solvers for the incompressible Navier–Stokes equations with volume-penalization: convergence of a dipole-wall collision *J. Comput. Phys.* **227** 919–45
- [31] Clercx H J H and Bruneau C-H 2006 The normal and oblique collision of a dipole with a no-slip boundary *Comput. Fluids* **35** 245–79
- [32] Schumacher J 2009 Lagrangian studies in convective turbulence *Phys. Rev. E* **79** 056301
- [33] Castaing B, Gunaratne G, Heslot F, Kadanoff L, Libchaber A, Thomae S, Wu X-Z, Zaleski S and Zanetti G 1989 Scaling of hard thermal turbulence in Rayleigh–Bénard convection *J. Fluid Mech.* **204** 1–30
- [34] Gasteuil Y, Shew W L, Gibert M, Chillá F, Castaing B and Pinton J-F 2007 Lagrangian temperature, velocity, and local heat flux measurement in Rayleigh–Bénard convection *Phys. Rev. Lett.* **99** 234302